Available online at www.sciencedirect.com
SCIENCE DIRECT®
Journal of Sound and Vibration 276 (2004) 1119–1127
JOURNAL OF SOUND AND VIBRATION
www.elsevier.com/locate/jsvi

Letter to the Editor

Experimental observation of non-linear effects in the propagation of a Friedlander pulse in a finite-length closed tube

W.J.N. de Lima[a,*], E.F. Vergara[a], R.S. Birch[b], S.N.Y. Gerges[a]

[a] *Laboratory of Industrial Noise, Mechanical Engineering Department, Federal University of Santa Catarina, Campus Universitario-Trindade, Florianopolis, SC, Cx Postal 476, Brazil*
[b] *Department of Engineering, Impact Research Center, University of Liverpool, Brownlow Hill, Liverpool L69 33GH, UK*

Received 10 October 2003; accepted 6 November 2003

1. Introduction

The theory of linear acoustics can only deal with waves of infinitesimal amplitudes and propagating a relatively short distance. As the wave amplitude and/or distance of propagation increase, the geometrical and physical non-linearities can greatly affect how the wave propagates in a medium, and phenomena such as shock formation and waveform distortion become important [1,2].

Most of the works on finite-amplitude plane waves in a tube deal with continuous waves. Pestorius and Blackstock [3] investigated sinusoidal wave and broadband acoustic noise in an infinite tube (finite tube with an anechoic termination). Nakamura et al. [4] presented a computational analysis of the waveform of plane N-waves in a circular tube and concluded that the slope of the straight-line segment of the waveform is affected by the non-linear distortion and the boundary layer dissipation.

One application of the study of finite-amplitude pulse propagation in a tube is to assess the performance of hearing protector devices (HPD) under intense impulsive noise (sound pressure level greater than 140 dB ref. 20 μPa) using objective methods [5]. This approach uses the non-linearity to create a train of pulses with different characteristics.

This paper aims at investigating the propagation of a finite-amplitude plane pulse inside a closed tube. More specifically, the paper investigates whether or not it is possible to simulate a tube with infinite length using a finite-length tube by verifying how the pulse distorts and if shocks form despite the dissipation and finite length. The distortion of the pulse is presented in time and frequency domain. Experimental results are explained based on the theory of non-linear acoustics.

*Corresponding author. Tel.: +55-48-3319227; fax: +55-48-2334455.
E-mail address: washdelima@hotmail.com (W.J.N. de Lima).

0022-460X/$ - see front matter
doi:10.1016/j.jsv.2003.11.028

2. Propagation of finite-amplitude plane pulse

The theory of non-linear acoustics deals with finite-amplitude waves. By finite-amplitude wave it means a wave with a small but larger than infinitesimal amplitude, such that the perturbation parameter, defined as the ratio of the particle velocity to sound propagation velocity, is yet infinitesimal. The effects of non-linearity are cumulative and even though the perturbation parameter is small, the non-linearity brings about phenomena such as waveform distortion and shock formation. Problems with very high amplitudes, such as in explosions, are out of the scope of non-linear acoustics and they are solved by the theory of compressible fluid dynamics. A comprehensive analysis and application of the theory of non-linear acoustics can be found in various books [1,2]. Here, only basic results of the propagation of finite-amplitude progressive plane waves are presented.

One of the most interesting characteristics of the non-linear wave propagation is the dependency of the sound velocity $c(x,t)$ on the local value of the amplitude of the wave [1,2],

$$c(x,t) = c_0 + (\beta - 1)u(x,t), \tag{1}$$

where β is the coefficient of non-linearity ($\beta = 1.2$ for air), c_0 is the small-amplitude sound speed ($c_0 = 343$ m/s for air), x is the position in the direction of propagation and $u(x,t)$ is the particle velocity. By disregarding local effects [1], the first order relation between excess pressure and particle velocity can be assumed ($p = \rho_0 c_0 u$) and therefore, Eq. (1) can be rewritten as

$$c(x,t) = c_0 + \frac{(\beta - 1)}{\rho_0 c_0} p(x,t) + O(\varepsilon^2), \tag{2}$$

where ρ_0 is the small-amplitude density and $\varepsilon = |u/c_0|$ is the perturbation parameter. Burgers equation is the simplest model that takes account of non-linear and dissipative aspects on the propagation of plane progressive waves:

$$\frac{\partial p}{\partial x} - \frac{\delta}{2c_0^3}\frac{\partial^2 p}{\partial \tau^2} = \frac{\beta p}{\rho_0 c_0^3}\frac{\partial p}{\partial \tau}, \tag{3}$$

where δ is the diffusivity of sound, $\tau = t - x/c_0$ is the retarded time. Disregarding attenuation ($\delta = 0$) and assuming a general source condition $p(0,\tau) = f(\tau)$, the exact solution of Eq. (3) is given by

$$p(x,t) = f\left(\tau + \frac{\beta p(x,\tau)}{\rho_0 c_0^3} x\right). \tag{4}$$

From Eq. (4) it is seen that the waveform peaks propagate faster than the waveform troughs due to the dependency of the solution on the local value of the amplitude of the wave (Eqs. (1) and (2)). Therefore, as the wave propagates, the waveform distorts and the wave becomes eventually very steep. There are distances where a discontinuity ($\partial p/\partial t = \infty$) appears in the solution (shock formation). The smallest distance where it occurs is called the shock distance formation $\bar{x}$ and it is defined as

$$\bar{x} = \frac{\rho_0 c_0^3}{\beta \max(\partial p/\partial \tau)}. \tag{5}$$

The solution given in Eq. (4) is valid only for a distance lower than the shock formation distance ($x<\bar{x}$). To describe the propagation after the shock distances ($x\geqslant\bar{x}$) the effect of dissipation must be taken into account.

3. Characterization of a pulse and a Friedlander pulse

Some quantities such as rise time, decay time, and total duration are necessary to qualify the pulses. These quantities are defined according to ISO 10843 [6]. The rise time t_{rise} is the time, in seconds, a signal takes to rise from 10% to 90% of its peak sound pressure, corresponding to the difference between t_1 and t_0 in Fig. 1. The maximum pressure P_0 is 80% of the peak pressure ($P_0 = 0.8P_{peak}$). The wavefront slope, s, is the ratio of maximum pressure and rise time, $s = P_0/t_{rise}$. The decay time t_{decay} is the time, in seconds, required for the pulse, after reaching its peak sound pressure, to decay from 90% to 10% of its peak sound pressure, corresponding to the difference between the times t_3 and t_2 in Fig. 1. The duration T is defined as the rise time plus six times the decay time. The duration represents the point at which the rarefaction of the pulse reaches asymptotically 1% of the peak pressure [7]. All these parameters are used in the next section to describe the distortion of the pulse when it propagates inside the tube.

4. Friedlander pulse

The experimental pulses are modelled as an ideal Friedlander pulse. The expression for the ideal Friedlander pulse is [8]

$$p(t) = \begin{cases} P_0(t/t_{rise}), & 0\leqslant t\leqslant t_{rise}, \\ P_0\left[1 - \dfrac{(t - t_{rise})}{t_{decay}}\right] e^{(t-t_{decay})/t_{decay}}, & t\geqslant t_{rise}. \end{cases} \tag{6}$$

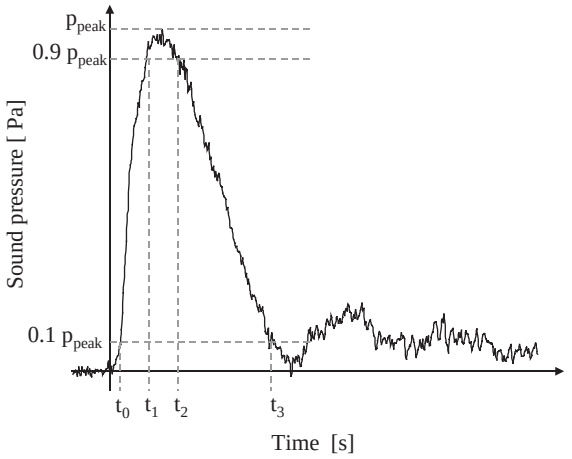

Fig. 1. Drawing showing a reverberating pulse with the temporal points used to define the rise time ($t_{rise} = t_1 - t_0$), decay time ($t_{decay} = t_3 - t_1$) and pulse duration ($T = t_{rise} + 6t_{decay}$).

Using Eq. (5), for this type of pulse the theoretical shock distance formation is

$$\bar{x} = \frac{\rho_0 c_0^3}{\beta} \frac{t_{rise}}{P_0}. \tag{7}$$

The distortion of a finite-amplitude propagating ideal Friedlander pulse can also be observed in the frequency domain by observing the changes in the spectrum. The Fourier transform of Eq. (6) is

$$P(\omega) = -\frac{1}{t_{rise}\omega^2} + \mathrm{e}^{-\mathrm{j}\omega t_{rise}} \frac{(1 - \omega^2 t_{decay}^2 - 2t_{rise}\omega^2 t_{decay}) + \mathrm{j}(2\omega t_{decay} + t_{rise}\omega)}{t_{rise}\omega^2[(1 - \omega^2 t_{decay}^2) + \mathrm{j}2\omega t_{decay}^2]}. \tag{8}$$

For $t_{rise} \ll t_{decay}$ and frequencies such that $\omega t_{decay} \gg 1$, an approximated expression for the spectral amplitude can be written as

$$|P(\omega)| = \frac{\sqrt{2}}{\omega^2 t_{rise}}[1 - \cos(\omega t_{rise})]^{1/2}. \tag{9}$$

From Eq. (9), two frequencies f_{rise} and f_{decay} named rise frequency and decay frequency, respectively, can be defined. The frequency f_{rise} is the point in the spectrum where the amplitude begin to decrease 12 dB/octav. The frequency f_{decay} is the point in the spectrum of maximum amplitude [8]. The frequencies f_{rise} and f_{decay} are related to t_{rise} and t_{decay} as [6]

$$f_{rise} = \frac{1}{3t_{rise}}, \quad f_{decay} = \frac{1}{2\pi t_{decay}}. \tag{10, 11}$$

Therefore, a waveform distortion is observed in the frequency domain by investigating the changes in the frequencies f_{rise} and f_{decay}.

5. Experiments and results

In the experiments, pulses were generated inside a closed tube and allowed to reverberate from end to end. A pulse generator [8] was connected to one end of a tube of 0.15 m diameter and 12.0 m long (Fig. 2). The other end of the tube was closed with an end-cap while the generator end, although not completely fixed, had a similarly behavior as a closed end [5]. Two

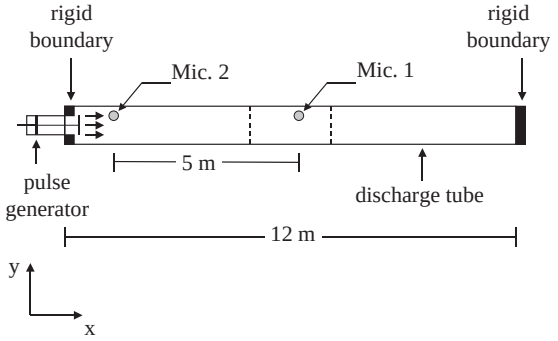

Fig. 2. Pulse generator with a tube of 150 mm diameter.

microphones, which were positioned at distances 1.0 and 6.0 m from the source in the wall of the tube, measured a train of pulses as multiple reflections of the primary Friedlander pulse occurred from end to end. The first microphone measured the initial pulse and the second microphone measured the pulse as it travelled back and forth inside the tube. The distance that the pulse travelled inside the tube is referred to as the accumulative distance of propagation. Three pulses were considered with approximately equal initial amplitudes ($P_0 = 158$ dB) but with varying initial rise times and durations (Table 1) and are named pulses A, B and C.

In Fig. 3 the train of waveforms of pulse B is presented. In this figure the first waveform is the initial pulse captured by the microphone fixed at 1.0 m ahead of the generator and the rest are reflections measured by the microphone at 6.0 m (Fig. 2). Similar trains of waveforms exist for pulses A and C.

As the pulses travelled inside the tube, their amplitudes decreased due to the thermo-viscous and boundary layer dissipative effects in the fluid and due to the radiation of energy through the wall and the ends of the tube. The peak-amplitudes of pulses A, B and C decayed linearly in a rate of 0.056, 0.09 and 0.20 dB/m, respectively. Therefore, the smaller the initial rise time, the higher the rate of attenuation (Fig. 4).

The distortion of the pulses is measured by the changing of the rise time (Fig. 5) or wavefront slope (Fig. 6) with respect to the accumulative distance. In the experimental results the wavefront slope reached a maximum (or rise time reaches a minimum) at a certain accumulative distance. This distance is named the experimental shock distance $\bar{x}_e$. The theoretical shock distance is given by Eq. (7) where the definition of P_0, t_{rise} and t_{decay} follows ISO 10843 [6] (see Section 3).

The values of theoretical experimental shock distance, $\bar{x}$ and $\bar{x}_e$, for all three pulses are presented in Table 2. There is a good agreement between the values of $\bar{x}$ and $\bar{x}_e$ for pulses B and C.

Table 1
Pulses A, B, and C with their respective initial maximum pressure P_0, initial rise time t_{rise}, and initial duration T

Pulse	P_0 (kPa)	P_0 (dB)	t_{rise} (ms)	T (ms)
A	1.6036	158.08	1.30	14.02
B	1.6962	158.57	0.70	10.90
C	1.7766	158.97	0.01	1.21

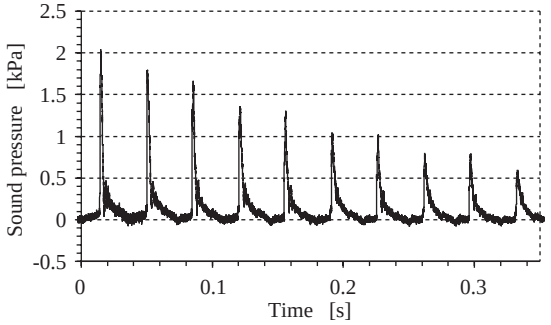

Fig. 3. Train of waveforms for pulse B.

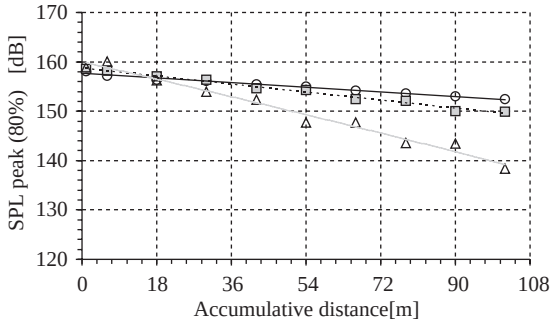

Fig. 4. The changing of the peak-amplitude pressure with the accumulative distance: ○, pulse A; ■, pulse B; △, pulse C.

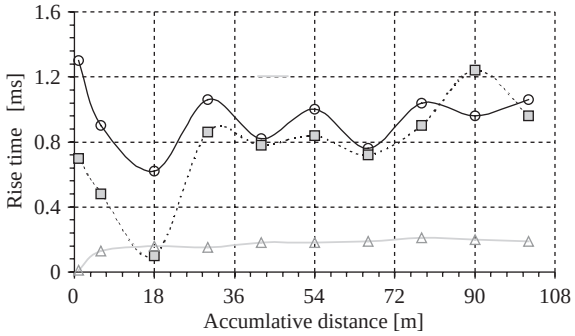

Fig. 5. The variation of rise time with the accumulative distance, key as in Fig. 4.

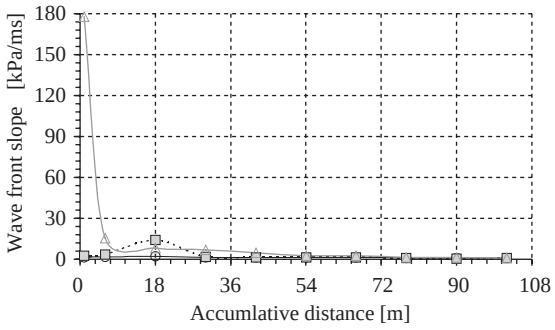

Fig. 6. The variation of wavefront slope with the accumulative distance, key as in Fig. 4.

Table 2
Pulses A, B, and C with their respective initial maximum pressure, theoretical shock distance $\bar{x}$ and experimental accumulative shock distance $\bar{x}_e$

Pulse	P_0 (kPa)	$\bar{x}$ (m)	$\bar{x}_e$ (m)
A	1.6036	33.28	18
B	1.6962	16.94	18
C	1.7766	0.23	1

The small difference between these values is due to the position of microphone 2 that did not necessarily coincide exactly with the position where the shock formed and also because the expression for $\bar{x}$ does not take in account the dissipative effects. Figs. 5 and 6 show that, although pulse A has high initial peak pressure (158.08 dB), it did not change very much its waveform (rise time or wavefront slope) as it propagated, and therefore, it did not become a shock wave. This phenomenon occurs because the non-linear effects (i.e., variation in the rise time) are overcome by the dissipative effects and, in turn, explain the poor agreement between $\bar{x}$ and $\bar{x}_e$ for this pulse (Table 2). Although the formation of shock is observed either from wavefront slope or rise time, Figs. 4 and 5 show that the wavefront slope is more sensitive to shock formation than it is to the rise time.

The ratio of the rise time to the duration is used to investigate the existence of a shock. Theoretically, shock forms when the ratio of the rise time to the duration is zero, but this criterion is never satisfied in an experiment. Hence, it is said that a shock has formed if the rise time is much smaller than the duration. Fig. 7 shows how the ratio of the rise time to the duration changes as the pulses propagate. Since pulses B and C became shock waves (Table 2), it is concluded that a shock formed when the rise time is smaller than 1% of the duration. Note that the minimum value of the ratio of the rise time to the duration of pulse A is around 4%, which corroborates the previous conclusion that pulse A never became, a shock wave.

Just after the shock there was a change in the rise time of pulse B (Fig. 5), which indicates that the shock wavefront was not sustained for long due to dissipation. However, the wavefront slope for pulse B reached a maximum again at an accumulative distance of propagation of 66.0 m, but at this distance the rise time did not reach a well-defined minimum and the ratio of the rise time to the duration was above 1%. Therefore, at 66.0 m the pulse B did not become a shock. In fact after 66.0 m the shock pulse B became a finite-amplitude pulse and eventually a linear pulse before it disappeared. Pulse C is generated as a shock wave but the shock wavefront disappeared quickly and the pulse propagated with constant rise time. This behavior of pulse C is due to its high rate of attenuation that consumes the discontinuity of the shock wavefront.

A similar analysis is done in the frequency domain. Table 3 presents f_{rise} and f_{decay} when the pulses A, B and C reached their smallest rise time. Figs. 8 and 9 show the changes of f_{rise} and f_{decay} with the accumulative distance. As is seen in the Fig. 9, the decay frequency (or decay time) did not change very much as the pulse propagates, and therefore, it did not inform when a shock forms.

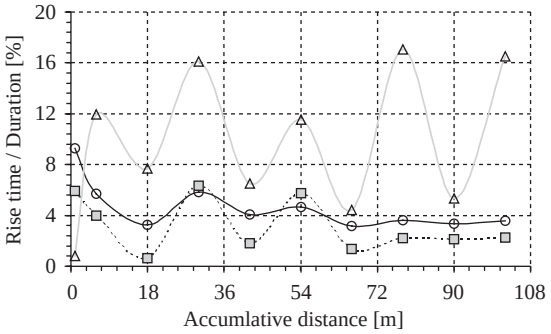

Fig. 7. The variation of the ratio of rise time to duration with accumulative distance, key as in Fig. 4.

Table 3
Pulses A, B, and C with their smallest rise time t_{rise} and the respective rise frequency f_{rise}, decay time t_{decay} and decay frequency f_{decay}

Pulse	$\bar{x}_e$ (m)	t_{rise} (ms)	f_{rise} (Hz)	f_{decay} (ms)	t_{decay} (Hz)
A	18	0.62	537.63	3.08	51.61
B	18	0.10	3334	2.70	58.95
C	1	0.01	33334	0.20	795.77

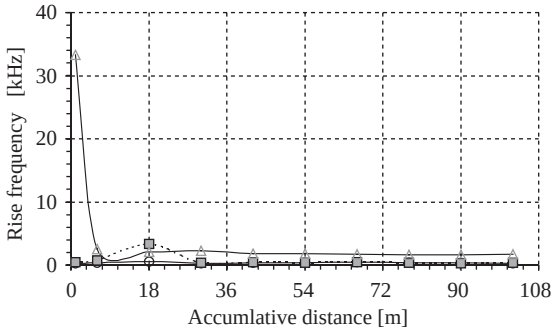

Fig. 8. The variation of rise frequency with accumulative distance, key as in Fig. 4.

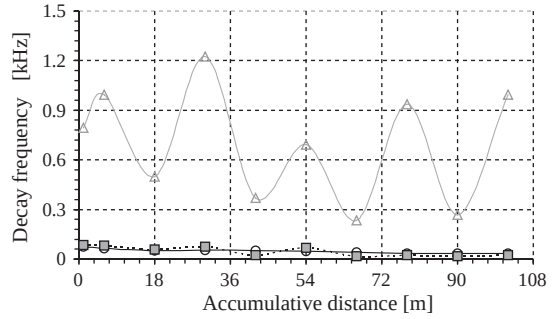

Fig. 9. The variation of decay frequency with accumulative distance, key as in Fig. 4.

6. Conclusion

The propagation of finite-amplitude plane pulse in a finite-length circular tube was investigated. The experimental results were explained in the light of non-linear acoustics. Due to the reflections on the ends of the tube, by generating only one pulse, it is possible to create a train of pulse, with different non-linear characteristics. Therefore, a finite-length closed tube can be used to simulate the propagation of a finite-amplitude pulse in an infinite tube. Shock waves form despite the dissipation and tube finite length. The rate of attenuation and distortion of the pulse with the distance depends upon the initial rise time and duration. The smaller the initial rise time, the higher the rate of attenuation. Although the formation of shock is observed either from wavefront slope or rise time, the wavefront slope is more sensitive to shock formation.

Acknowledgements

The authors wish to acknowledge the support of the Conselho Nacional de Desenvolvimento Científico e Tecnológico (CNPq) of Brazil.

References

[1] D.T. Blackstock, M.F. Hamilton (Eds.), *Nonlinear Acoustics*, Academic Press, Boston, 1998.
[2] K. Naugolnykh, L. Ostrovsky, *Nonlinear Wave Processes in Acoustics*, Cambridge Texts in Applied Mathematics, Cambridge University Press, Cambridge, 1998.
[3] F.M. Pestorius, D.T. Blackstock, Propagation of finite-amplitude noise, in: L. Bjørnø (Ed.), *Finite-Amplitude Wave Effects in Fluids*, IPC Science and Technology Press, Guildford, Surrey, UK, pp. 24–29.
[4] A. Nakamura, R. Takeuchi, S. Oie, Nonlinear attenuation of an N wave propagation in a tube, including dissipation due to wall effects, *Journal of the Acoustical Society of America* 63 (2) (1978) 346–352.
[5] R.S. Birch, S.N. Gerges, E.F. Vergara, Design of a pulse generator and shock tube for measuring hearing protector attenuation of high-amplitude impulsive noise, *Applied Acoustic* 64 (3) (2003) 269–286.
[6] International Organization for Standard ISO 10843. Acoustics—Methods for the Description and Physical Measurement of Single Impulses or Series of Impulses, International Standard, 1997.
[7] R.P. Hamernik, D. Hsueh, Impulse noise: some definitions, physical acoustics and other considerations, *Journal of the Acoustical Society of America* 90 (1) (1991) 189–196.
[8] F.G. Friedlander, *Sound Pulses*, Cambridge University Press, Cambridge, 1958.